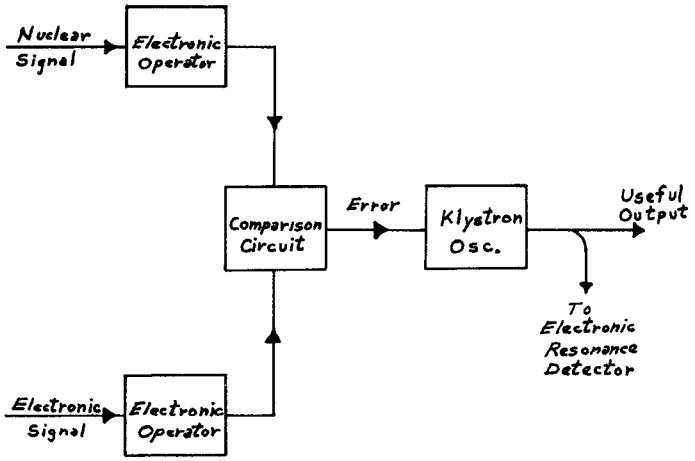

Fig. 8—AFC system using simultaneous resonance.

rect the microwave frequency for simultaneity. A strong electronic resonance signal may be observed with only 100 microwatts of microwave power leaving the major portion of the klystron power for useful output. The blocks marked electronic operator prepare the resonance signals so they may be fed into a phase detector and thus give rise to an error signal.

Limitations

The major limitation on the accuracy of measurement or control is the natural resonance line width of the electron resonance. One of the substances giving the strongest electron resonance is diphenyl-trinitrophenyl-hydrazyl with a line width of 2.7 Gauss. On the assumption that the center one tenth of this curve could be located, an accuracy of 1 part in 10^4 could be obtained. Another factor contributing to inaccuracy is magnetic field homogeneity. All of the sample must see the same field strength else the resonance line will be broadened beyond its natural width. Good field homogeneity may be insured by careful alignment of the pole faces and by using a large ratio of pole diameter to gap distance. Careful shimming of the pole face will also improve field homogeneity. Fields more homogeneous than one part in 10^6 over a square centimeter are difficult to attain because of local inhomogeneities in the magnetic properties of the pole face material.

Narrow electron resonance lines may be obtained from the electrons in an electron beam which is made to interact with the microwave field. Line widths of the order of 0.5 Gauss have been reported by this method giving a frequency ratio accurate to one part in 10^5. The narrowest electron resonance to come to our attention is that of a solution of sodium in ammonia with a half maximum width of 0.08 Gauss. This electron resonance used with a water proton resonance might give rise to control accuracies of one part in 10^6, depending on the signal to noise ratio for the electron resonance and the field homogeneity.

The observed width of the proton resonance in water is usually due to the magnetic field inhomogeneity as it has been possible to obtain in fields of 7000 Gauss proton resonance curves with a line width of 0.001 Gauss. This corresponds to a resolution of one part in 7 million.

Discontinuities in a Rectangular Waveguide Partially Filled with Dielectric*

CARLOS M. ANGULO†

Summary—The modal spectrum for a rectangular waveguide with a dielectric slab at the bottom of the guide is obtained following the Characteristic Green's Function method developed by Marcuvitz. Then a four-terminal network is found as equivalent to the junction of the partially filled waveguide and an empty rectangular waveguide.

An integral equation is written for the electric field at the plane of the junction and variational expressions are derived for the parameters of the four-terminal network connecting the transmission line equivalent to the partially filled waveguide to the transmission line equivalent to the empty guide.

A reasonable guess for the electric field at the discontinuity gives approximate values for the parameters of the four-terminal network. These values agree with experiment.

The parameters of the network are plotted vs frequency and thickness of the slab.

* Manuscript received by PGMTT, June 20, 1956.
† Brown University, Providence, R. I.

Introduction

A CONSIDERABLE AMOUNT of literature has been devoted recently to surface waves. The reader is referred to van Bladel and Higgins[1] for an introduction to the effect of dielectrics in rectangular waveguides and to Barlow and Cullen[2] for surface waves in dielectric slabs. The main purpose of this paper is to obtain a four-terminal network equivalent to the junction of an empty rectangular waveguide and a rectangular waveguide partially filled with dielectric. The Schwinger variational principle combined with the

[1] J. van Bladel and T. J. Higgins, "Cut-off frequency in two-dielectric layered rectangular wave guides," *J. App. Phys.*, vol. 22, p. 329; March, 1951.
[2] H. M. Barlow and A. L. Cullen, "Surface waves," *Proc. IEE*, Part III, vol. 100, p. 329; November, 1953.

modal analysis and synthesis technique developed by Marcuvitz give excellent results in our problem and encouraged the author to extend the method to the open-dielectric slab as reported in another paper.[3] In the methods used in this paper it is important to know the mode spectrum in the partially-filled guide as well as to be sure of the completeness of the mode spectrum. Therefore a systematic method of finding the modes is also given in this paper. This is the Characteristic Green's Function method given by Marcuvitz[4] which yields the modes he gave in his communication to the annual meeting of the Physical Society in 1952.

The geometry of the partially-filled waveguide allows us to separate the characteristic modes into two groups (see Fig. 1):

E_y modes, for which $H_y = 0$ and

H_y modes, for which $E_y = 0$.

Let us assume that the launching of energy in one or both of the waveguides of Fig. 1 is such that only E_y modes are excited. Under these circumstances only E_y modes will be present in both guides. We will not mention this fact again and it will be understood that we refer only to E_y modes throughout this paper.

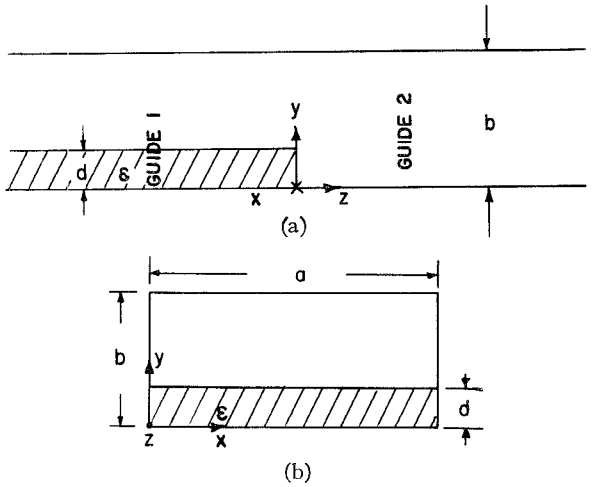

Fig. 1—(a) Longitudinal section of the junction; (b) cross section of waveguide 1.

The Characteristic Modes of the Partially-Filled Guide

The direction of propagation is OZ. We will refer to the projection of each field on the XOY plane as the transverse component and we will represent it with the subscript t.

The transversal component of the fields can be represented as follows:

$$\vec{E}_t(x, y, z) = \sum_{n,m} V_{n,m}(z)\vec{e}_{n,m}(x, y) \tag{1}$$

$$\vec{H}_t(x, y, z) = \sum_{n,m} I_{n,m}(z)\vec{h}_{n,m}(x, y). \tag{2}$$

The set of characteristic E_y modes is a complete orthonormal set. In order to satisfy Maxwell's equations, the following relations should hold:

$$\vec{h}_{n,m}(x, y) = \phi_n(x)\psi_m(y)\vec{x}_0 \tag{3}$$

$$0 = \left(\frac{d^2}{dx^2} + \zeta_n^2\right)\phi_n(x) \tag{4a}$$

$$\phi_n(0) = \phi_n(a) = 0 \tag{4b}$$

$$0 = \left[\epsilon(y)\frac{d}{dy}\frac{1}{\epsilon(y)}\frac{d}{dy} + \eta_m^2\right]\psi_m(y) \tag{5a}$$

$$\left[\frac{d\psi_m}{dy}\right]_{y=0} = \left[\frac{d\psi_m}{dy}\right]_{y=b} = 0 \tag{5b}$$

$$\vec{e}_{n,m} = -\frac{1}{\omega Z_{n,m}\mathcal{K}_{n,m}}\left[\frac{K^2 - \eta_m^2}{\epsilon(y)}\vec{y}_0 + \frac{1}{\epsilon(y)}\frac{\partial^2}{\partial x \partial y}\vec{x}_0\right]\phi_n(x)\psi_m(y) \tag{6}$$

$$\frac{dV_{n,m}(z)}{dz} = -jZ_{n,m}\mathcal{K}_{n,m}I_{n,m}(z) \tag{7a}$$

$$\frac{dI_{n,m}(z)}{dz} = -jY_{n,m}\mathcal{K}_{n,m}V_{n,m}(z) \tag{7b}$$

where $\vec{x}_0$ and $\vec{y}_0$ are the unit vectors in the OX and OY directions; ζ_n, η_m, $\mathcal{K}_{n,m}$ are the propagation wave-number in the OX, OY and OZ directions; $\epsilon(y)$ is the relative permittivity; $K^2 = \omega^2\mu_0\epsilon_0\epsilon(y)$ is the propagation wave-number of a plane wave in the direction perpendicular to the front wave; μ_0 and ϵ_0 are the permeability and permittivity of vacuum. Finally

$$Z_{n,m} = \frac{1}{Y_{n,m}} = \frac{\mathcal{K}_{n,m}}{\omega\epsilon_0} \tag{8}$$

is defined as the characteristic impedance of the waveguide for the n, m mode.

It is clear that for one given mode the propagation wave numbers ζ_n and $\mathcal{K}_{n,m}$ are the same in both media. However, η_m will have different values in the dielectric and in the air.

The solutions of (4) are obviously proportional to

$$\sin\frac{n\pi_x}{a}. \tag{9}$$

The solution of (5) is more complicated because of the variation of $\epsilon(y)$. We proceed to find the function $\psi_m(y)$ by the Characteristic Green's Function method. This method is most advantageous, since it leads directly to the completeness relation

$$\epsilon(y)\delta(y - y') = \sum_m \psi_m(y)\psi_m(y'). \tag{10}$$

For an explanation of the method in general, see Marcuvitz.[4] In our case we have to solve

[3] C. M. Angulo, "Diffraction of surface waves by a semi-infinite dielectric slab," IRE Trans., vol. AP-5, no. 1; January, 1957.
[4] N. Marcuvitz, "Field Representations in Spherically Stratified Regions," N.Y.U. Res. Rep. No. En-29, 1951.

$$\left[\frac{d}{dy}\frac{1}{\epsilon(y)}\frac{d}{dy}+\frac{p(y)}{\epsilon(y)}\right]G(y, y', p) = -\delta(y-y') \quad (11a)$$

$$\left[\frac{dG}{dy}\right]_{y=0} = \left[\frac{dG}{dy}\right]_{y=b} = 0 \quad (11b)$$

where $\delta(y-y')$ is the Dirac's delta function and G is the Characteristic Green's Function. $p(y)$ is equal to the square of the propagation wave number in the OY direction; *i.e.*, $p(y)=\eta^2$.

Since

$$\epsilon(y) = \begin{cases}\epsilon & d<y<b \\ 1 & 0<y<d\end{cases} \quad (12)$$

$p(y)$ will also take two constant values.

For one mode

$$\omega^2\mu_0\epsilon_0 = K_0^2 = \zeta_n^2 + \eta^2_{m(\text{air})} + \mathfrak{K}^2_{n,m} \quad (13a)$$

$$\omega^2\mu_0\epsilon_0\epsilon = K^2 = \zeta_n^2 + \eta^2_{m(\text{diel})} + \mathfrak{K}^2_{n,m}. \quad (13b)$$

Therefore the two values that $p(y)$ takes are

$$p(y) = \begin{cases}p' = p + K_0^2(\epsilon-1) & d<y<b \\ p & 0<y<d.\end{cases} \quad (14)$$

The solution for (11) is

$$G(y, y', p) = -\frac{\left[\cos\sqrt{p'}(y_> - d) + \epsilon\frac{\sqrt{p}}{\sqrt{p'}}\tan\sqrt{p}(b-d)\sin\sqrt{p'}(y_>-d)\right]\frac{\cos\sqrt{p'}y_<}{\cos\sqrt{p'}d}}{\sqrt{p}\tan\sqrt{p}(b-d)+\frac{\sqrt{p'}}{\epsilon}\tan\sqrt{p'}d} \quad \text{for } \begin{matrix}0<y<d\\0<y'<d\end{matrix} \quad (15)$$

and

$$G(y, y', p) = -\frac{\left[\cos\sqrt{p}(y_< - d) - \frac{\sqrt{p'}}{\epsilon\sqrt{p}}\tan\sqrt{p'}d\sin\sqrt{p}(y_<-d)\right]\frac{\cos\sqrt{p}(y_>-b)}{\cos\sqrt{p}(b-d)}}{\sqrt{p}\tan\sqrt{p}(b-d)+\frac{\sqrt{p'}}{\epsilon}\tan\sqrt{p'}d} \quad \text{for } \begin{matrix}d<y<b\\d<y'<b.\end{matrix} \quad (16)$$

The symbol $y_<$ stands for y or y', whichever is smaller, and $y_>$ for whichever is larger.

If we consider now the constant p as a complex variable, we have

$$\epsilon(y)\delta(y-y') = -\frac{1}{2\pi j}\int G(y, y', p)dp. \quad (17)$$

The integration must be done counterclockwise around all the singularities of $G(y, y', p)$ in the p plane.

In the present situation the singularities are only an infinite discrete set of poles along the real axis (Fig. 2).

These poles are the values of p for which

$$\sqrt{p}\tan\sqrt{p}(b-d)+\frac{\sqrt{p'}}{\epsilon}\tan\sqrt{p'}d = 0 \quad (18a)$$

$$p'-p = K_0^2(\epsilon-1). \quad (18b)$$

These values of p give the resonances of the system or the characteristic modes of the partially-filled guide.

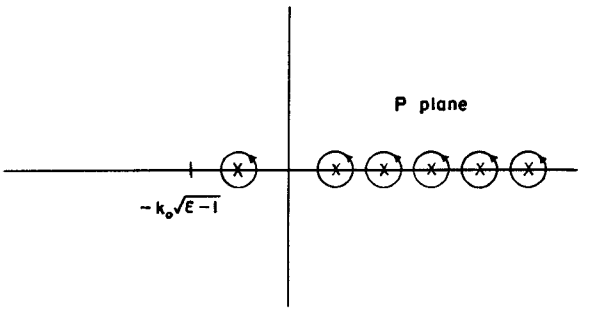

Fig. 2

The normalized mode spectrum in the y direction is then given as minus the summation of all the residues of $G(y, y', p)$. The residues of (15) give the $\psi_m(y)$ for $0<y<d$ and the residues of (16) give the functions $\psi_m(y)$ for $d<y<b$ (Fig. 1).

Eq. (18) has solutions for which

$$K_0 < p < K_0\sqrt{\epsilon}. \quad (19)$$

These modes have sinusoidal variation in the dielectric ($0<y<d$) and hyperbolic variation in the air. They are the surface waves and the number of them that the partially-filled guide can support depends on the frequency and thickness of the slab. The lowest of these surface waves has no cut-off frequency. We will assume in this paper that the frequency is such that the structure has only one surface wave among its characteristic modes. Fig. 3 plots $\eta_{(\text{diel})}$ and $j\eta_{(\text{air})}$ vs K_0d for different values of the relative permittivity ϵ for the only surface wave in our case. Fig. 4 is the plot of $\mathfrak{K}$.

Eq. (18) has also solutions for which

$$K_0 < K_0\sqrt{\epsilon} < p. \quad (20)$$

These modes have sinusoidal variation in the OY direction in both regions, dielectric and air. For the wavelength of the excitation in this paper ($\lambda=3.2$ cm) these are nonpropagating modes. Figs. 5 to 8 (p. 72) are the plots for $\eta_{(\text{air})}$ and $\eta_{(\text{diel})}$ for the first five modes of this type and $\epsilon=2.49$.

Finally, the mode functions are obtained as follows:

$$\vec{h}^{\{\text{air}\}}_{n,m}(x, y) = \vec{x}_0 B^{\{\text{air}\}}_{n,m}\sin\frac{n\pi}{a}x\cos\eta^{\{\text{air}\}}_m\begin{Bmatrix}y-b\\ y\end{Bmatrix} \quad (21a)$$

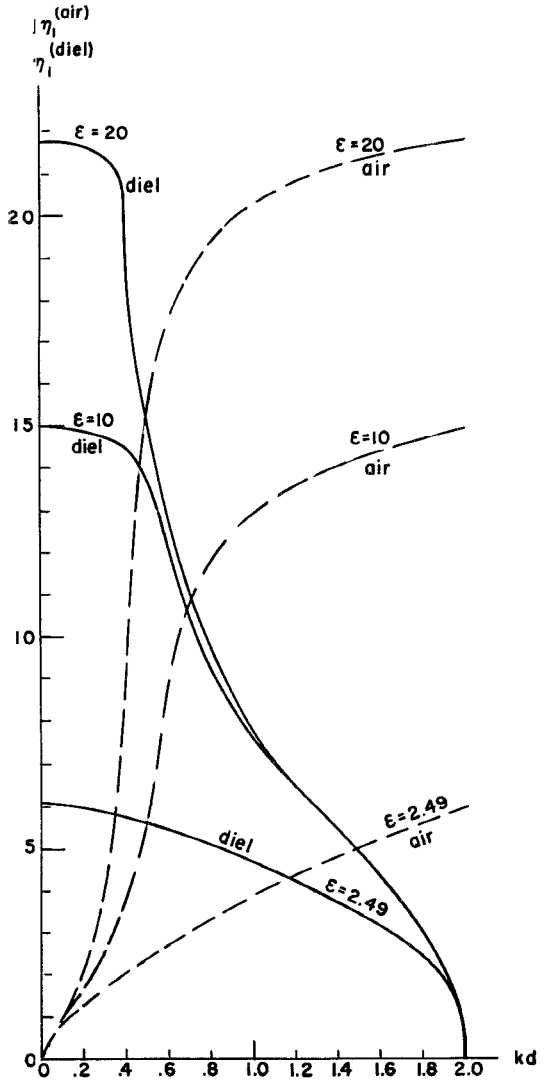

Fig. 3—Propagation wave number in the OY direction for the propagating mode (slow wave).

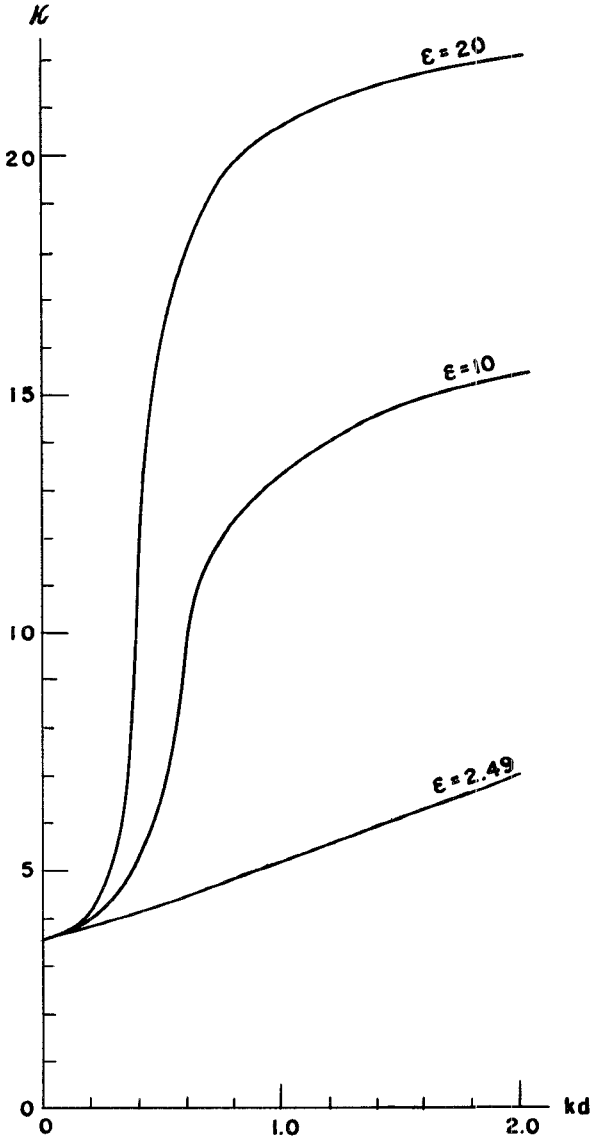

Fig. 4—Propagation wave number in the OZ direction for the propagating mode (slow wave).

$$\overrightarrow{e}_{n,m}^{\{\substack{\text{air}\\\text{diel}}\}}(x, y) = \frac{-B_{n,m}^{\{\substack{\text{air}\\\text{diel}}\}}}{\omega Z_{n,m}\mathcal{K}_{n,m}}\left[\frac{\mathcal{K}_{n,m}^2 + \left(\frac{n\pi}{a}\right)^2}{\left\{\begin{matrix}1\\ \epsilon\end{matrix}\right\}}\overrightarrow{y_0}\sin\frac{n\pi}{a}x\cos\eta_m^{\{\substack{\text{air}\\\text{diel}}\}}\left\{\begin{matrix}y-b\\ y\end{matrix}\right\} - \frac{\frac{n\pi}{a}\eta_m^{\{\substack{\text{air}\\\text{diel}}\}}}{\left\{\begin{matrix}1\\ \epsilon\end{matrix}\right\}}\overrightarrow{x_0}\cos\frac{n\pi}{a}x\sin\eta_m^{\{\substack{\text{air}\\\text{diel}}\}}\left\{\begin{matrix}y-b\\ y\end{matrix}\right\}\right]. \quad (21b)$$

The normalization constant is chosen such that

$$\int_0^b dy\int_0^a \overrightarrow{z_0}\times\overrightarrow{e}_{n,m}(x, y)\cdot\overrightarrow{h}_{n,m}(x, y)dx = 1 \quad (22)$$

and its value is

$$B_{n,m}^{(\text{diel})} \doteq \frac{2\sqrt{\frac{\epsilon}{ad}}\,\frac{\mathcal{K}_{n,m}}{\sqrt{\mathcal{K}_{n,m}^2 + \left(\frac{n\pi}{a}\right)^2}}}{\left\{1 + \frac{\sin 2\eta_m^{(\text{diel})}d}{2\eta_m^{(\text{diel})}d} + \frac{\cos^2\eta_m^{(\text{diel})}d}{\cos^2\eta_m^{(\text{air})}(b-d)}\,\epsilon\,\frac{b-d}{d}\left[1 + \frac{\sin 2\eta_m^{(\text{air})}(b-d)}{2\eta_m^{(\text{air})}(b-d)}\right]\right\}^{1/2}} \quad (23a)$$

$$B_{n,m}^{(\text{air})} = \frac{\eta_m^{(\text{diel})}}{\eta_m^{(\text{air})}}\;\frac{\cos\eta_m^{(\text{diel})}d}{\cos\eta_m^{(\text{air})}(b-d)}\,B_{n,m}^{(\text{diel})}. \quad (23b)$$

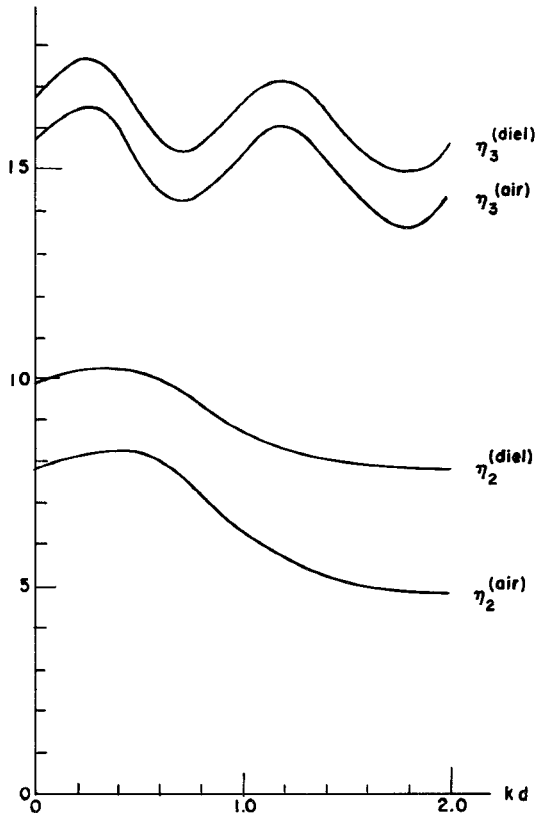

Fig. 5—Propagation wave number in the OY direction for the first two nonpropagating modes.

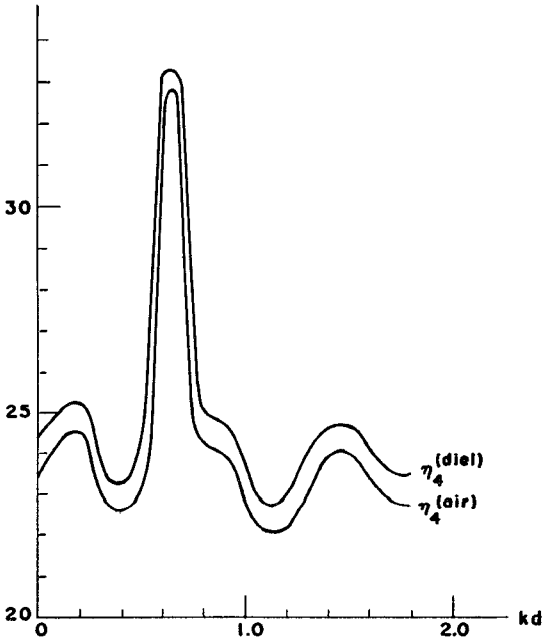

Fig. 6—Propagation wave number in the OY direction for the third nonpropagating mode.

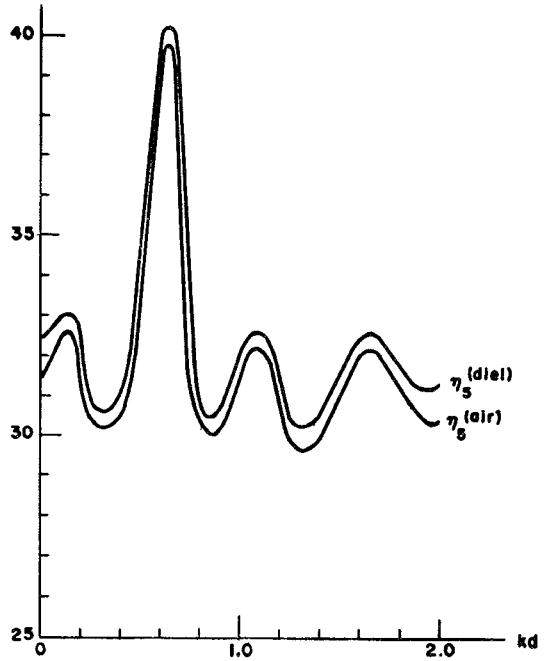

Fig. 7—Propagation wave number in the OY direction for the fourth nonpropagating mode.

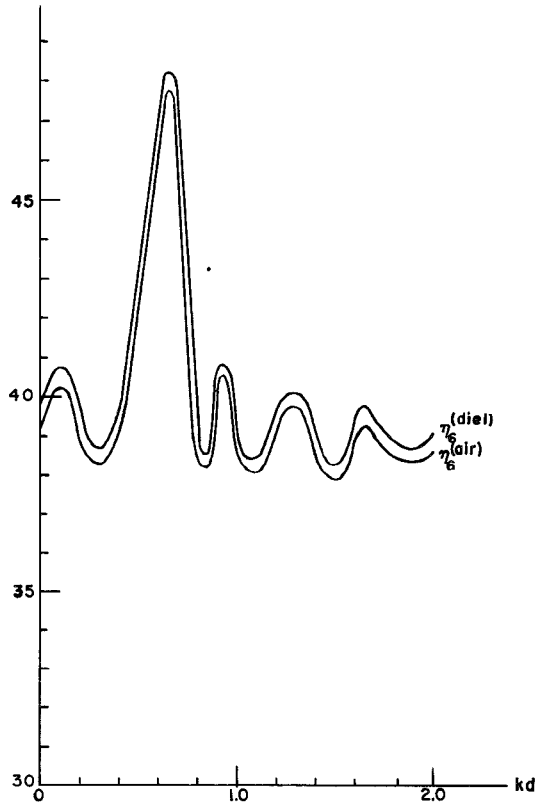

Fig. 8—Propagation wave number in the OY direction for the fifth nonpropagating mode.

The Four-Terminal Network Equivalent to the Discontinuity

In the empty rectangular waveguide we use a representation similar to the one described previously. It is well known and we will not write any details here.

Let us represent the transversal magnetic field $\vec{H}_t$ at the junction of the two guides in terms of the characteristic modes of guide 1 and in terms of those of guide 2. We can equate the two representations, since the transversal magnetic field is continuous at $z=0$. Therefore:

$$I_1^{(1)}(0)\vec{h}_1^{(1)}(x, y) - \sum_n{}' Y_n^{(1)}V_n^{(1)}(0)\vec{h}_n^{(1)}(x, y)$$

$$= -I_1^{(2)}(0)\vec{h}_1^{(2)}(x, y) + \sum_m{}' Y_m^{(2)}V_m^{(2)}(0)\vec{h}_m^{(2)}(x, y) \quad (24)$$

where the upper index refers to waveguide 1 or 2 in Fig. 1, the summations are actually double summations and only for convenience we have indicated the mode with only one subindex. In (24) we have also assumed that each guide propagates only the lowest mode and we have separated these modes from the summations and indicated them with the subindex 1. The prime in the summations indicates that the first or lowest mode is excluded.

In view of the orthogonality properties (22) and of (1) and (2) we can write (24) as follows:

$$I_1^{(1)}(0)\vec{h}_1^{(1)}(x, y) + I_1^{(2)}(0)\vec{h}_1^{(2)}(x, y) = \int_0^b dy' \int_0^a \overleftrightarrow{\mathcal{Y}}(x, y; x', y') \times \vec{z}_0 \cdot \vec{E}_t(x', y')dx'. \quad (25)$$

In (25) we have written the dyadic $\overleftrightarrow{\mathcal{Y}}$ which has the following meaning

$$\overleftrightarrow{\mathcal{Y}}(x, y; x', y') = \sum_n{}' Y_n^{(1)}\vec{h}_n^{(1)}(x, y)\vec{h}_n^{(1)}(x', y') + \sum_m Y_m^{(2)}\vec{h}_m^{(2)}(x, y)\vec{h}_m^{(2)}(x', y'). \quad (26)$$

Eq. (25) is the integral equation for the electric field at the discontinuity. We cannot solve it exactly but we can use the Schwinger variational principle for the unknown electric field.

If the unknown field is written as follows:

$$\vec{E}_t(x, y) = I_1^{(1)}(0)\vec{\mathcal{E}}_1(x, y) + I_1^{(2)}(0)\vec{\mathcal{E}}_2(x, y). \quad (27)$$

One arrives at the following relations

$$V_1^{(1)}(0) = Z_{11}I_1^{(1)}(0) + Z_{12}I_1^{(2)}(0) \quad (28a)$$

$$V_1^{(2)}(0) = Z_{21}I_1^{(1)}(0) + Z_{22}I_1^{(2)}(0) \quad (28b)$$

which link the dominant modes in the two guides replacing the effect of the discontinuity by a four-terminal network. The expressions for the impedances are stationary and can be calculated with a small error without knowing the exact field at $z=0$.

$$\frac{1}{Z_{22}} = \frac{\int_0^b\int_0^a dxdy\vec{z}_0\times\vec{\mathcal{E}}_2(x, y)\cdot\int_0^b\int_0^a dx'dy'\overleftrightarrow{\mathcal{Y}}(x, y; x', y')\cdot\vec{z}_0\times\vec{\mathcal{E}}_2(x', y')}{\left[\int_0^b\int_0^a \vec{z}_0\times\vec{\mathcal{E}}_2(x, y)\cdot\vec{h}_1^{(2)}(x, x)dxdy\right]^2} \quad (29a)$$

$$\frac{1}{Z_{12}} = \frac{\int_0^b\int_0^a dxdy\vec{z}_0\times\vec{\mathcal{E}}_2(x, y)\cdot\int_0^b\int_0^a dx'dy'\overleftrightarrow{\mathcal{Y}}(x, y; x', y')\cdot\vec{z}_0\times\vec{\mathcal{E}}_1(x', y')}{\int_0^b\int_0^a z_0\times\vec{\mathcal{E}}_2(x, y)\cdot\vec{h}_1^{(1)}(x, y)dxdy\int_0^b\int_0^a \vec{z}_0\times\vec{\mathcal{E}}_1(x', y')\cdot\vec{h}_1^{(2)}(x', y')dx'dy'} \quad (29b)$$

$$\frac{1}{Z_{11}} = \frac{\int_0^b\int_0^a dxdy\vec{z}_0\times\vec{\mathcal{E}}_1(x, y)\cdot\int_0^b\int_0^a dx'dy'\overleftrightarrow{\mathcal{Y}}(x, y; x', y')\cdot\vec{z}_0\times\vec{\mathcal{E}}_1(x', y')}{\left[\int_0^b\int_0^a \vec{z}_0\times\vec{\mathcal{E}}_1(x, y)\cdot\vec{h}_1^{(2)}(x, y)dxdy\right]^2}. \quad (29c)$$

The above expressions are minima for the exact field. Of all the approximations tried one of them gives a very convergent series and the smallest value for the admittance. Two points measured experimentally agree within 5 per cent with the curve for $1/Z_{22}$ vs K_0d. The approximation consists of taking the field of the dominant mode in the empty waveguide as the field at the discontinuity, *i.e.*:

$$\vec{\mathcal{E}}_1(x, y) = \vec{\mathcal{E}}_2(x, y) = \vec{e}_1^{(2)}(x, y). \quad (30)$$

If one substitutes into (29) and performs the necessary integrations one obtains

$$\frac{Z_{1,0}^{(1)}}{Z_{22}} = \sum_{m=2}^{\infty} M_m^2 \quad (31a)$$

$$\sqrt{\frac{Z_{1,1}^{(1)}Z_{1,0}^{(2)}}{Z_{12}}} = \frac{1}{M_1}\sum_{m=2}^{\infty} M_m^2 \quad (31b)$$

$$\frac{Z_{1,1}^{(1)}}{Z_{11}} = \frac{1}{M_1^2}\sum_{m=2}^{\infty} M_m^2 \quad (31c)$$

where

$$M_m = \frac{1}{\sqrt{1-\left(\frac{\lambda}{2a}\right)^2}}\sqrt{\frac{a}{2b\mathcal{C}_{1,m}^{(1)}}}\frac{B_{1,m}^{(\text{diel})}}{\eta_m^{(\text{diel})}}\left\{1-\left[\frac{\eta_m^{(\text{diel})}}{\eta_m^{(\text{air})}}\right]^2\frac{1}{\epsilon}\right\}\sin\eta_m^{(\text{diel})}d. \quad (32)$$

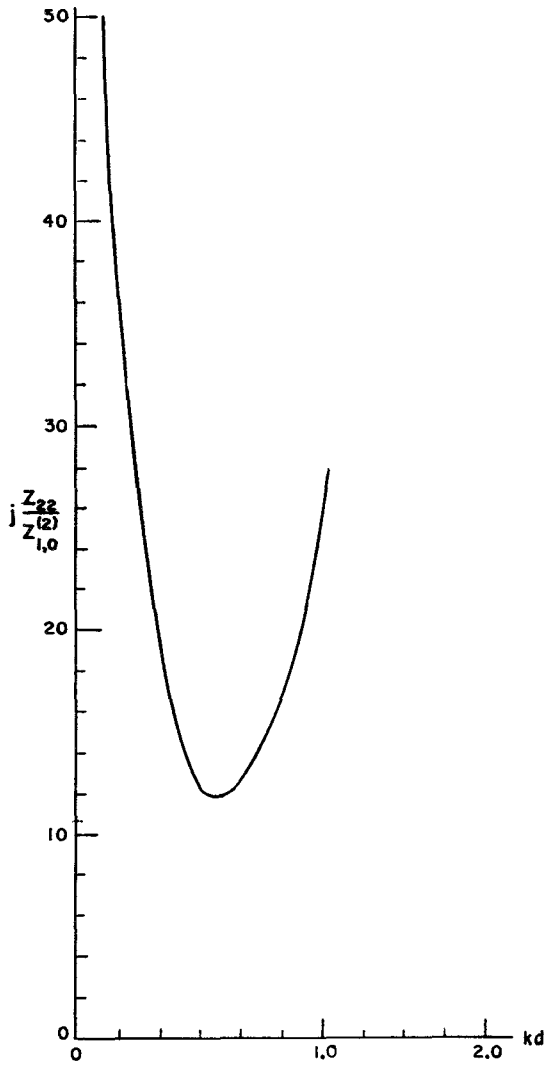

Fig. 9—(a) Shunt impedance offered by the discontinuity; (b) transformer ratio.

The series converges very rapidly and only five terms are necessary. $B_{1,m(\text{diel})}$ is given in (23a); η_m is plotted in Figs. 5–8 for $m=2$, 3, 4, 5 and in Fig. 3 for $m=1$.

Fig. 9 is a plot of

$$j\frac{Z_{22}}{Z_{1,0}^{(2)}} \text{ and } n=\frac{1}{M_1}\sqrt{\frac{Z_{1,0}^{(2)}}{Z_{1,1}^{(1)}}} \text{ vs } K_0 d$$

for an X-band rectangular waveguide, for $\lambda=3.2$ cm and $\epsilon=2.49$.

Eq. (31) indicates that we can replace the discontinuity by the four-terminal network of Fig. 10, a pure

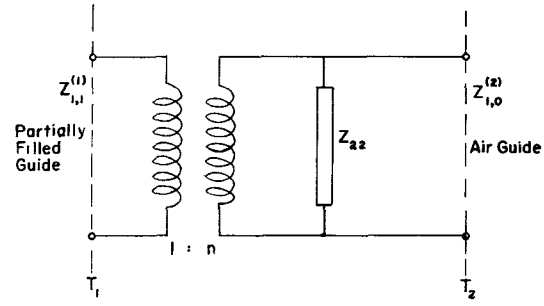

Fig. 10—Circuit equivalent to the discontinuity.

shunt and an ideal transformer with the following transform ratio:

$$n^2=\frac{Z_{22}}{Z_{11}}=\frac{1}{M_1^2}\frac{Z_{1,0}^{(2)}}{Z_{1,1}^{(1)}}.$$

The reference planes are at the plane of the discontinuity $z=0$ in Fig. 1.

Acknowledgment

The main results of this paper were obtained while the author was at the Polytechnic Institute of Brooklyn; the paper was presented as a thesis for the Master's degree in electrical engineering. The guidance of Professor Marcuvitz is gratefully acknowledged. The author wishes also to express his thanks to Professor Ernst Weber for lending the facilities of the Microwave Research Institute for the experimental measurements and computations. Additional computations and the final publication form have been possible through Contract AF 19(604)-1391 between Cambridge Air Force Research Center and Brown University.